

## Wannier excitons in low-dimensional microstructures: Shape dependence of the quantum size effect

Yosuke Kayanuma

*Department of Physics, Faculty of Science, Tohoku University, Sendai 980, Japan*

(Received 26 July 1991)

The shape dependence of the quantum size effect of the Wannier exciton is clarified by a simple variational calculation for a model of microcrystal with cylindrical shape. According to the change of the ratio of the radius of the section and the length of the cylinder to the effective Bohr radius of the exciton, the motional state of the exciton changes from three-dimensional to quasi-two-, one-, and zero-dimensional. It is shown that when there is a large anisotropy in the shape of the microstructure, the spatial extension of the exciton wave function along the relatively free coordinate shrinks from the bulk value, reflecting the low dimensionality due to the strong confinement along the axis perpendicular to it.

Recently, the optical properties of low-dimensional semiconductor microstructures have attracted much interest. The exciton state in these systems can be strongly modified from that in the bulk materials due to the spatial confinement of the wave function. This is called the quantum size effect (QSE). The QSE becomes salient when the characteristic linear dimension of the microstructure is reduced to the value comparable to the effective Bohr radius of the exciton  $a_B^*$ . For example, the changeover from the three-dimensional exciton to a quasi-two-dimensional one was clearly observed in the absorption spectra of the GaAs thin films.<sup>1</sup> It has been pointed out that the low-dimensional modification of the exciton is advantageous for application to optical devices<sup>2,3</sup> and recent research activities extend further to the microfabrication of even lower-dimensional microstructures such as quantum wires<sup>4</sup> and quantum dots.<sup>5</sup>

There is another recent topic on mesoscopic systems called microcrystals.<sup>6</sup> The microcrystal is the analog of the quantum dots but, at present, one can attain one or two orders of magnitude smaller size by various growth techniques of the microcrystals than by the microfabrication of the quantum dots. In the theoretical analysis of the QSE in microcrystals, the shape of the microcrystals is regarded as approximately spherical<sup>7,8</sup> although in some materials the shape is highly anisotropic.

The QSE of the Wannier exciton is strongly dependent on the shape or the dimensionality of the microstructure. In view of the rapid development of the crystal growth and microfabrication techniques, it will be worthwhile to

make clear the shape dependence of the QSE from a unified standpoint. As a step toward this goal, I discuss here this problem with the variational calculation in a simplified model system.

Consider an electron and a hole confined in a microcrystal of cylindrical shape with the radius of the horizontal section  $R$  and the length  $L$  as shown in Fig. 1. By changing the values of  $R/a_B^*$  and  $L/a_B^*$ , we can systematically study the change of the motional state of the exciton between various limiting situations, namely, the limit of three dimension (the bulk crystal) for  $R/a_B^* \gg 1$  and  $L/a_B^* \gg 1$ , the quasi-two-dimension (the quantum well) for  $R/a_B^* \gg 1$  and  $L/a_B^* \lesssim 1$ , the one dimension (the quantum wire) for  $R/a_B^* \lesssim 1$  and  $L/a_B^* \gg 1$ , and the zero dimension (the quantum dot) for  $R/a_B^* \lesssim 1$  and  $L/a_B^* \lesssim 1$ . We adopt the effective-mass approximation with the isotropic effective mass  $m_e$  and  $m_h$  for the electron and the hole, respectively. For simplicity, the penetration of the wave function outside the microcrystal and the distortion of the Coulomb interaction due to the difference of the dielectric constants between the microcrystal and the matrix are neglected here.

The coordinates of the electron and the hole are denoted as  $(\mathbf{r}_e, z_e)$  and  $(\mathbf{r}_h, z_h)$ , respectively, where  $\mathbf{r}_i$  is the two-dimensional vector in the horizontal section and  $z_i$  is the value of the  $z$  axis. In order to study the lowest state, it is expedient to adopt the coordinate system,  $r_e \equiv |\mathbf{r}_e|$ ,  $r_h \equiv |\mathbf{r}_h|$ ,  $r_{eh} \equiv |\mathbf{r}_e - \mathbf{r}_h|$ . The Hamiltonian is then given by

$$H = -\frac{\hbar^2}{2m_e} \left[ \frac{\partial^2}{\partial r_e^2} + \frac{1}{r_e} \frac{\partial}{\partial r_e} + \frac{r_e^2 - r_h^2 + r_{eh}^2}{r_e r_{eh}} \frac{\partial^2}{\partial r_e \partial r_{eh}} + \frac{\partial^2}{\partial z_e^2} \right] - \frac{\hbar^2}{2m_h} \left[ \frac{\partial^2}{\partial r_h^2} + \frac{1}{r_h} \frac{\partial}{\partial r_h} + \frac{r_h^2 - r_e^2 + r_{eh}^2}{r_h r_{eh}} \frac{\partial^2}{\partial r_h \partial r_{eh}} + \frac{\partial^2}{\partial z_h^2} \right] - \frac{\hbar^2}{2\mu} \left[ \frac{\partial^2}{\partial r_{eh}^2} + \frac{1}{r_{eh}} \frac{\partial}{\partial r_{eh}} \right] - \frac{e^2}{\epsilon [r_{eh}^2 + (z_e - z_h)^2]^{1/2}}, \quad (1)$$

where  $\mu \equiv 1/(m_e^{-1} + m_h^{-1})$  is the reduced mass and  $\epsilon$  is the dielectric constant. As for the trial wave function, we choose

$$\Psi(r_e, r_h, r_{eh}, z_e, z_h) = NJ_0(\gamma r_e)J_0(\gamma r_h)\cos(\pi z_e/L)\cos(\pi z_h/L)\exp\{-\alpha[r_{eh}^2 + (z_e - z_h)^2]^{1/2}\}, \quad (2)$$

which satisfies the boundary condition that  $\Psi$  should vanish at  $r_e = R, r_h = R, z_e = \pm L/2$ , and  $z_h = \pm L/2$ . In the above equation,  $J_0$  is the zeroth-order Bessel function with  $\gamma = 2.40483/R$ ,  $N$  is the normalization constant, and  $\alpha$  is the variational parameter which determines the spatial extension of the internal motion of the exciton.

The variational principle requires one to minimize

$$E(R, L) \equiv \int_0^R dr_e \int_0^R dr_h \int_{|r_e - r_h|}^{r_e + r_h} dr_{eh} \int_{-L/2}^{L/2} dz_e \int_{-L/2}^{L/2} dz_h W(r_e, r_h, r_{eh}) \Psi^*(r_e, r_h, r_{eh}, z_e, z_h) H \Psi(r_e, r_h, r_{eh}, z_e, z_h), \quad (3)$$

under the normalization condition, where the weight  $W(r_e, r_h, r_{eh})$  is given by

$$W(r_e, r_h, r_{eh}) = 4\pi r_e r_h r_{eh} / \{[(r_e + r_h)^2 - r_{eh}^2][(r_e - r_h)^2 - r_{eh}^2]\}^{1/2}. \quad (4)$$

By introducing the variables  $\tau \equiv z_e + z_h$ ,  $\sigma \equiv z_e - z_h$ , the integration over  $\tau$  can be carried out analytically and the integration over the remaining four variables was carried out numerically.

In the limit  $L/a_B^* \rightarrow \infty$ , our model reduces to that of Brown and Spector.<sup>9</sup> They showed how the exciton binding energy increases from the three-dimensional value in the limit  $R/a_B^* \rightarrow \infty$  to the one-dimensional value in the limit  $R/a_B^* \rightarrow 0$ . As is well known, the binding energy of the one-dimensional exciton diverges.<sup>10</sup> As  $R/a_B^*$  decreases, the optimizing value of  $\alpha$  once decreases slightly from the bulk value  $a_B^{*-1}$  and then increases to infinity in the limit  $R/a_B^* \rightarrow 0$ . On the other hand, in the limit  $R/a_B^* \rightarrow \infty$ , the model reduces to that studied by Bastard *et al.*<sup>11</sup> The binding energy increases from the three-dimensional value in the limit  $L/a_B^* \rightarrow \infty$  to the two-dimensional value in the limit  $L/a_B^* \rightarrow 0$ . The two-dimensional exciton has a binding energy four times larger than the three-dimensional value. The parameter  $\alpha$  increases from  $a_B^{*-1}$  to  $2a_B^{*-1}$  as  $L/a_B^*$  decreases from  $\infty$  to 0. Our variational function (2) bridges these two limiting cases. Note that the term "binding energy" has well-defined meaning only when  $R/a_B^* \rightarrow \infty$  and/or  $L/a_B^* \rightarrow \infty$ .

Let us see how the energy and the wave function of the exciton changes as  $L/a_B^*$  is decreased from  $\infty$  to 0 for fixed values of  $R/a_B^*$ . Roughly speaking, this corresponds to observing the change from the three dimension to the two dimension in the case  $R/a_B^* \gg 1$  and from the one dimension to the zero dimension in the case  $R/a_B^* \ll 1$ . In Fig. 2, the energy shift  $\Delta E(R, L) \equiv E(R, L) - E(R, \infty)$  due to the confinement along the

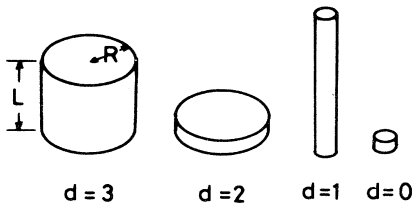


FIG. 1. Illustration of the dimensionality  $d$  of the microcylinder model.

axis of the cylinder is plotted against  $L/a_B^*$  with the effective rydberg energy  $E_{Ry}^*$  as the unit of energy. For a fixed value of  $L/a_B^*$ ,  $\Delta E(R, L)$  becomes much smaller for smaller values of  $R/a_B^*$  because of the compactness of the quasi-one-dimensional exciton.

The dimensionality-dependent changeover of the exciton state is clearly seen in Fig. 3 where the optimizing value of  $\alpha$  is plotted against  $L/a_B^*$  for fixed values of  $R/a_B^*$ . For  $R/a_B^* = 10$ ,  $\alpha$  increases roughly from the three-dimensional value  $\alpha \approx a_B^{*-1}$  to the two-dimensional value  $\alpha \approx 2a_B^{*-1}$  as  $L/a_B^*$  is decreased from  $\infty$  to 0. On the other hand, in the case  $R/a_B^* = 0.1$ ,  $\alpha$  decreases from the quasi-one-dimensional value ( $\alpha \approx 1.86a_B^{*-1}$  in this case) for  $L/a_B^* \rightarrow \infty$  to nearly zero as  $L/a_B^*$  is decreased. Every curve takes the minimum value at around  $L \approx 2R$  and tends to the value for the strictly two-dimensional flat disk at  $L/a_B^* = 0$ . The present author<sup>12</sup> studied the

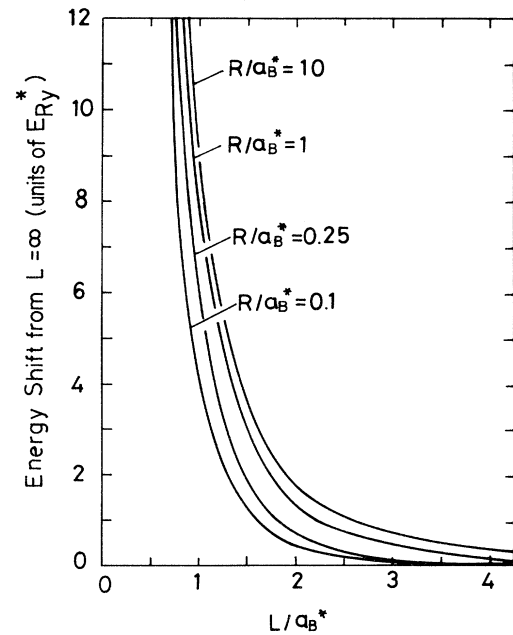


FIG. 2. High-energy shift  $\Delta E(R, L) \equiv E(R, L) - E(R, \infty)$  of the lowest state of the exciton in the microcylinder due to the confinement along the axis.

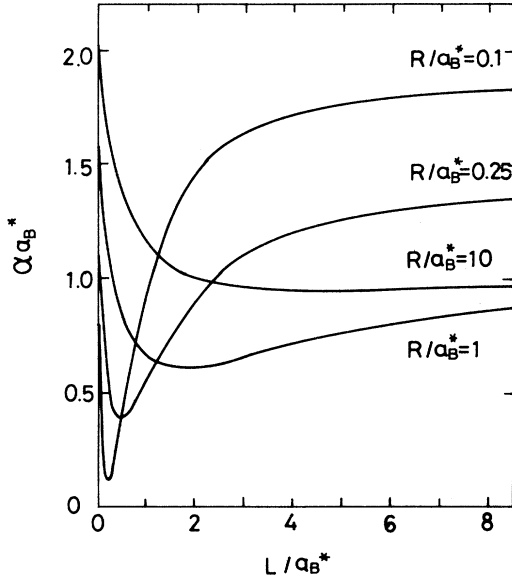


FIG. 3. The optimizing value of  $\alpha$  plotted against the normalized length  $L$  with the normalized radius  $R$  as a fixed parameter.

QSE in a spherical microcrystal with the same type of variational wave function as Eq. (2). In that case,  $\alpha$  decreases monotonously from the three-dimensional value  $\alpha = a_B^{*-1}$  to the zero-dimensional exact value  $\alpha = 0.4980 \dots a_B^{*-1}$  as  $R/a_B^*$  tends to 0.

The longitudinal and the transverse extension of the wave function are calculated as

$$\bar{z}_{eh} \equiv [\langle \Psi | (z_e - z_h)^2 | \Psi \rangle]^{1/2} \quad (5)$$

and

$$\bar{r}_{eh} \equiv (\langle \Psi | r_{eh}^2 | \Psi \rangle)^{1/2}, \quad (6)$$

respectively. In Fig. 4,  $\bar{r}_{eh}/a_B^*$  is plotted against  $L/a_B^*$ .

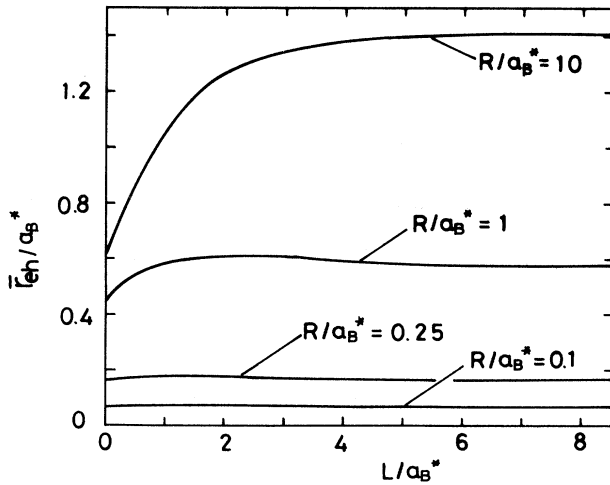


FIG. 4. Normalized transverse extension of the internal motion of the exciton in the microcylinder.

The curve for  $R/a_B^* = 10$  almost coincides with that calculated by Bastard *et al.*<sup>11</sup> for  $R/a_B^* = \infty$ . Namely, it interpolates the limiting values of the three dimension  $\bar{r}_{eh} = \sqrt{2}a_B^*$  for  $L/a_B^* \rightarrow \infty$ , and the two dimension  $\bar{r}_{eh} = \sqrt{3/8}a_B^*$  for  $L/a_B^* \rightarrow 0$ . In the limit of thin wire  $R/a_B^* \ll 1$ ,  $\bar{r}_{eh}$  tends to the asymptotic value  $0.69R$  independently of  $L/a_B^*$ , which is the value for the uncorrelated motion of the electron and the hole in the plane perpendicular to the axis of the wire.

In Fig. 5,  $\bar{z}_{eh}/a_B^*$  is plotted against  $L/a_B^*$ . The curve for  $R/a_B^* = 10$  extrapolates to the three-dimensional value  $\bar{z}_{eh} = a_B^*$  for  $L/a_B^* \rightarrow \infty$ . In the limit of thin slab  $L/a_B^* \ll 1$ ,  $\bar{z}_{eh}$  tends to the asymptotic value  $(1/6 - \pi^{-2})^{1/2}L \simeq 0.255 \dots L$  independently of  $R/a_B^*$ , which is the value for the uncorrelated motion of the electron and the hole in the direction perpendicular to the surface of the slab. Note that for  $R/a_B^* \ll 1$ ,  $\bar{z}_{eh}$  becomes small and rather unaffected by the confinement in the  $z$  direction even for relatively small values of  $L/a_B^*$ .

From Figs. 4 and 5, we find a general correlation between the internal motion of the Wannier exciton and the anisotropy in the shape of the confining microstructure. Namely, when there is a large anisotropy, the spatial extension along the relatively free coordinate shrinks from the bulk value due to the strong confinement along the coordinate perpendicular to it. The spatial correlation between the electron and the hole along the latter coordinate becomes weaker while that along the former even stronger.

The oscillator strength of the optical transition per unit volume  $f_1$  for the lowest state normalized by that of the bulk exciton  $f_{ex}$  is given by the formula<sup>13</sup>

$$f_1/f_{ex} = \frac{\pi a_B^{*3}}{V} \left| \int \Psi(r, r, 0, z, z) dV \right|^2, \quad (7)$$

where the factor proportional to the photon energy is neglected. In Fig. 6, the calculated  $f_1/f_{ex}$  is shown. See how the low-dimensionality enhances the oscillator strength per unit volume.

A little care must be taken in evaluating the asymptotic value of  $f_1$  in the limit  $L/a_B^* \rightarrow \infty$ . In the case

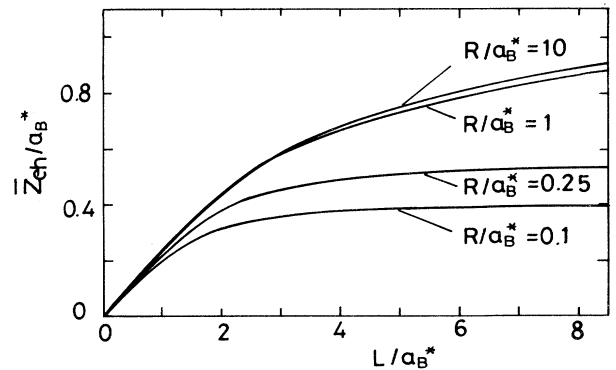


FIG. 5. Normalized longitudinal extension of the internal motion of the exciton.

$L/a_B^* \gg 1$ , the confinement condition along the  $z$  axis can be approximately considered to work on the translational degree of freedom to the exciton in this direction. The low-lying eigenstates are then specified by the sub-band index  $n(=1,2,3,\dots)$  for the center-of-mass motion together with the quantum numbers specifying the internal motion. The oscillator strength  $f_n$  for the  $n$ th sub-band with the lowest internal eigenstate is then given by

$$f_n \approx \frac{8}{(2n+1)^2} \frac{1}{\pi^2} \tilde{f}, \quad n=1,2,3,\dots \quad (8)$$

where  $\tilde{f}$  is the oscillator strength of the corresponding eigenstate for the cylinder with the infinite length. It should be noted that  $f_1$  does not tend to  $\tilde{f}$  but tends to  $0.81\tilde{f}$  even in the limit  $L/a_B^* \rightarrow \infty$ : The oscillator strength for the lowest eigenstate in the infinite cylinder is distributed to the closely lying excited states of the center-of-mass motion. (Note that  $\sum_{n=1}^{\infty} f_n = \tilde{f}$ .) This leads to a somewhat paradoxical situation in the emission spectrum since the transition probability does not tend to that of the infinite cylinder in the limit  $L/a_B^* \rightarrow \infty$ . The same argument also works in the confinement along the direction perpendicular to the axis. An analogous phenomenon has also been noted in the QSE of microspheres.<sup>7,8</sup>

The spatial extension of the internal motion of the exciton has an importance in determining the physical quantities such as the exchange splitting or the diamagnetic shift. Recently, optical investigations of the microcrystals of anisotropic materials such as  $\text{PbI}_2$  (Ref. 14) and  $\text{BiI}_3$  (Ref. 15) have been carried out. Their shapes are regarded as slabs or thin disks rather than spheres. In addition, the effective masses  $m_e$  and  $m_h$  are also strongly anisotropic in these materials. The analysis of the experimental data of these anisotropic microcrystals with the

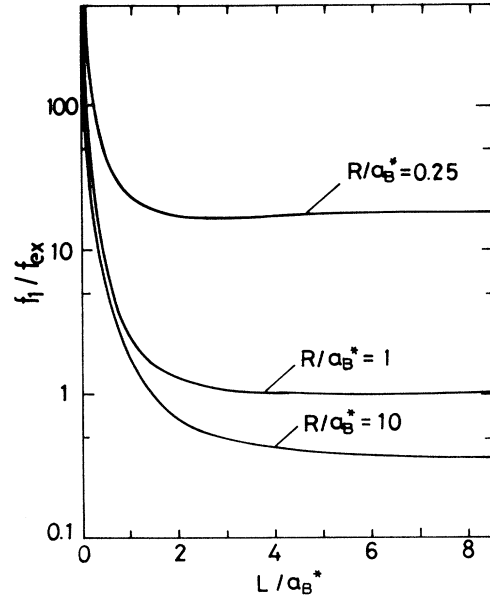


FIG. 6. The oscillator strength per unit volume normalized by that of the bulk exciton.

extension of the present model will be presented elsewhere.

The author would like to thank Professor T. Goto, Professor T. Komatsu, and Professor T. Iida for valuable discussions and information. This work was partially supported by a Grant-in-Aid from the Ministry of Education of Japan.

<sup>1</sup>R. D. Dingle, W. Wiegman, and C. H. Henry, *Phys. Rev. Lett.* **33**, 827 (1974).

<sup>2</sup>Y. Arakawa and H. Sakaki, *Appl. Phys. Lett.* **40**, 939 (1982).

<sup>3</sup>S. Smidt-Rink, D. A. B. Miller, and D. S. Chemla, *Phys. Rev. B* **35**, 8113 (1986); E. Hanamura, *ibid.* **38**, 1228 (1988).

<sup>4</sup>P. M. Petroff, A. C. Gossard, R. A. Logan, and W. Wiegman, *Appl. Phys. Lett.* **41**, 635 (1982); J. Cibert and P. M. Petroff, *Phys. Rev. B* **36**, 3243 (1987); E. Kapan, S. S. Simhony, R. Bhat, and D. M. Haug, *Appl. Phys. Lett.* **55**, 2715 (1989).

<sup>5</sup>H. Temkin, G. J. Dolan, M. B. Panish, and S. N. G. Chu, *Appl. Phys. Lett.* **50**, 413 (1987); J. Cibert, P. M. Petroff, G. J. Dolan, S. J. Pearton, A. C. Gossard, and J. H. English, *ibid.* **49**, 1275 (1986); Y. Miyamoto, M. Cao, Y. Shingai, K. Furuya, Y. Suematsu, K. G. Ravikumar, and S. Arai, *Jpn. J. Appl. Phys.* **26**, L225 (1987).

<sup>6</sup>See, for instance, Y. Wang, and N. Herron, *J. Phys. Chem.* **95**,

525 (1991), and references therein.

<sup>7</sup>A. L. Efros and A. L. Efros, *Fiz. Tekh. Poluprovodn.* **16**, 1209 (1982) [*Sov. Phys.—Semicond.* **16**, 7 (1982)].

<sup>8</sup>Y. Kayanuma, *Phys. Rev. B* **38**, 9797 (1988).

<sup>9</sup>J. W. Brown and H. N. Spector, *Phys. Rev. B* **35**, 3009 (1987). See also T. Kodama, Y. Osaka, and M. Yamanishi, *Jpn. J. Appl. Phys.* **24**, 1370 (1985); L. Banyai, I. Galbraith, C. Ell, and H. Haug, *Phys. Rev. B* **36**, 6099 (1987).

<sup>10</sup>R. Loudon, *Am. J. Phys.* **44**, 1064 (1976).

<sup>11</sup>G. Bastard, E. E. Mendez, L. L. Chang, and L. Esaki, *Phys. Rev. B* **26**, 1974 (1982).

<sup>12</sup>Y. Kayanuma, *Solid State Commun.* **59**, 405 (1986).

<sup>13</sup>C. H. Henry and K. Nassau, *Phys. Rev. B* **1**, 1628 (1969).

<sup>14</sup>T. Goto, S. Saito, and M. Tanaka, *Solid State Commun.* (to be published).

<sup>15</sup>T. Komatsu (private communication).